

Electronic Supporting Information

Double-twist Pyridine-Carbonitrile Derivatives Enabling Excellent Thermally Activated Delayed Fluorescence Emitters for High-performance OLEDs

Jiafang Li,^a Wen-Cheng Chen,^b He Liu,^{*a} Zhanxiang Chen,^c Danyang Chai,^a Chun-Sing Lee,^{*b} Chuluo Yang^{*ac}

^a Shenzhen Key Laboratory of Polymer Science and Technology, Guangdong Research Center for Interfacial Engineering of Functional Materials, College of Materials Science and Engineering, Shenzhen University, Shenzhen 518060, Peoples's Republic of China E-mail: liuhe001@szu.edu.cn, clyang@szu.edu.cn

^b Center of Super-Diamond and Advanced Films (COSDAF) and Department of Chemistry, City University of Hong Kong, Kowloon, Hong Kong SAR 999077, P.R. China. E-mail: C.S.Lee@cityu.edu.hk

^c Department of Chemistry, Hubei Key lab on Organic and Polymeric Optoelectronic Materials, Wuhan University, Wuhan 430072, Peoples's Republic of China

General information

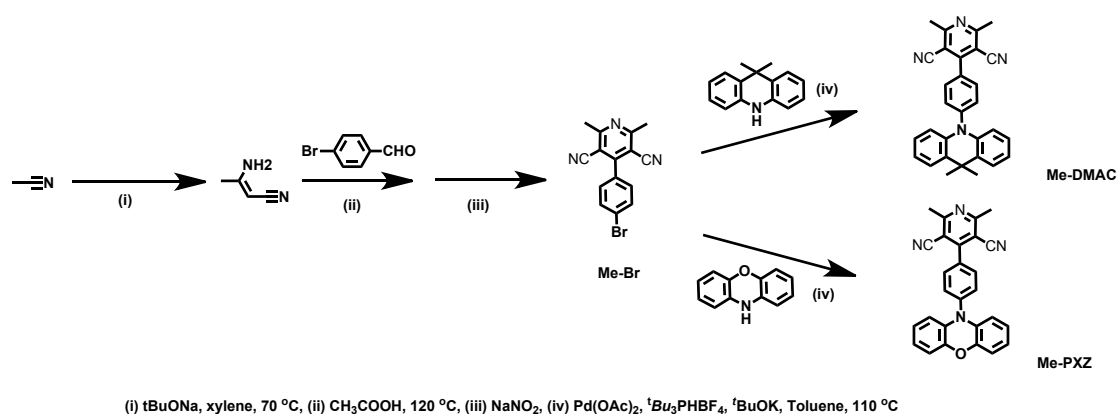
All oxygen- and moisture-sensitive manipulations were carried out under an inert atmosphere. All the chemicals were purchased from commercial sources and used as received unless stated otherwise. Toluene was refluxed over Na and distilled under dry argon. Synthesized compounds were subject to purification by temperature gradient sublimation in high vacuum before used in subsequent studies. The 500 MHz ^1H and 126 MHz ^{13}C NMR spectra were recorded on a Bruker Ascend 500 spectrometer using CDCl_3 as solvent and tetramethylsilane (TMS) as an internal reference. Mass analyses were recorded by Bruker autoflex MALDI-TOF mass spectrometer. UV-Vis absorption spectra were recorded on a Shimadzu UV-2700 recording spectrophotometer. Photoluminescence (PL) spectra were recorded on a Hitachi F-4600 fluorescence spectrophotometer. Phosphorescence spectra of thin films were conducted at 77K. Thermogravimetric analysis (TGA) was recorded on a TA Q50 instrument under nitrogen atmosphere at a heating rate of $10^\circ\text{C}/\text{min}$ from 25°C to 800°C . The temperature of degradation (T_d) was correlated to a 5% weight loss. Differential Scanning Calorimetry were carried out on a TA Q200. The glass transition temperature (T_g) was determined from the second heating scan at a heating rate of $10^\circ\text{C min}^{-1}$ from 25 to 250°C . Cyclic voltammetry (CV) was carried out in nitrogen-purged tetrahydrofuran or acetonitrile (reduction scan) or dichloromethane (oxidation scan) at room temperature with a CHI voltammetric analyzer. Tetrabutylammonium hexafluorophosphate (0.1 M) was used as the supporting electrolyte. The conventional three-electrode configuration consisted of a platinum working electrode, a platinum

wire auxiliary electrode and an Ag wire pseudo-reference electrode with ferroceniumferrocene (Fc^+/Fc) as the internal standard. Cyclic voltammograms were obtained at scan rate of 100 mV/s. Formal potentials were calculated as the average of cyclic voltammetric anodic and cathodic peaks. The HOMO energy levels of the compounds were calculated according to the formula: $-[4.8 + (E_{1/2}(\text{ox/red}) - E_{1/2}(\text{Fc}/\text{Fc}^+))]$ eV. The onset potential was determined from the intersection of two tangents drawn at the rising and background current of the cyclic voltammogram. The PL lifetimes were measured by a single photon counting spectrometer from Edinburgh Instruments (FLS920) with a Picosecond Pulsed UV-LASTER (LASTER377) as the excitation source. The samples were placed in a vacuum cryostat chamber with the temperature control. The solid state absolute PLQYs were measured on a Quantaurus-QY measurement system (C9920-02, Hamamatsu Photonics) equipped with a calibrated integrating sphere in the host of mCP (10 wt%) and all the samples were excited at 330 nm. During the PLQY measurements, the integrating sphere was purged with pure and dry argon to maintain an inert environment. The ground state molecular structures were optimized at the B3LYP-D3(BJ)/def2-SVP level and B3LYP/6-31G** level of theory; the S_1 and T_1 geometries were optimized via time-dependent DFT (TDDFT) at B3LYP/6-31G** level of theory. In addition, the overlaps between the hole and electron density distributions in the S_1 and T_1 states were estimated by the Multiwfn code.

Device Fabrication

Pre-cleaned indium tin oxide coated glass substrates with a sheet resistance of 15 Ω per square used as a transparent anode, then subjected to UV-ozone treatment for 15 min and transferred to a vacuum deposition system with a base pressure of approximately 10^{-6} Torr. The organic layers are deposited on the ITO substrates with an evaporation rate around 1-2 \AA s^{-1} . While, the cathode layers of LiF and Al are completed by thermal deposition at rates of 0.1 \AA s^{-1} and 10 \AA s^{-1} , respectively. Electroluminescence spectra and the corresponding luminance were recorded using PMA-12 photonic multichannel analyzer (Hamamatsu), and the current density-voltage-luminance characteristics were measured by computer controlled Keithley 237 power source (Tektronix) under ambient atmosphere.

Synthesis of Me-DMAC and Me-PXZ



Scheme S1 synthetic route of Me-DMAC and Me-PXZ.

Synthesis of 3-aminobut-2-enitrile

A solution of 100 ml xylene and 14.6 g (130 mmol) potassium t-butoxide were loaded in a 250 ml three-necked round bottom flask and heated to 70 $^{\circ}\text{C}$. A solution of 13 ml (250 mmol) acetonitrile with 15 ml xylene was added dropwise. Then the reaction was

mechanically stirring overnight. After cooled down to room temperature, saturate NaHCO_3 was added and stirred for another 30 min. Organic phase were separated and evaporated to get crude product 6 g. Yield: 58.4%. The product was used without further purification. ^1H NMR (CDCl_3 , 500 MHz) δ (ppm): 4.69 (2 H, s), 3.84 (1 H, s), 1.94 (3 H, s).

Synthesis of 4-(4-bromophenyl)-2,6-dimethylpyridine-3,5-dicarbonitrile (Me-Br)

6 g (73 mmol) 3-aminobut-2-enenitrile and 5.4 g (29.2 mmol) 4-bromobenzaldehyde were mix with 50 ml acetate acid and reflux overnight. After cooled to 75 °C, 20 g (292 mmol) sodium nitrite was added portionwise to the reaction and stirred for another 1 h at 75 °C. 150 ml water were used to quench the reaction and the pale white precipitate was filtered off followed by washed with water and dried at 60 °C overnight. (8.3 g, Yield: 91.1%). ^1H NMR (CDCl_3 , 500 MHz) δ (ppm): 7.74-7.72 (2 H, d, J 8.5), 7.41-7.39 (2 H, d, J 8.5), 2.87 (6 H, s). ^{13}C NMR (126 MHz, CDCl_3) δ (ppm): 165.33, 155.56, 132.57, 131.72, 130.25, 126.04, 114.99, 107.15, 24.71.

Synthesis of 4-(4-(9,9-dimethylacridin-10(9*H*)-yl)phenyl)-2,6-dimethylpyridine-3,5-dicarbonitrile (Me-DMAC)

Me-DMAC was synthesized via Buckwald-Hartwig coupling reaction. Me-Br (624 mg, 2 mmol), 9,9-dimethyl-9,10-dihydroacridine (460 mg, 2.2 mmol), Palladium (II) acetate (22.4 mg, 0.1 mmol), tri-*tert*-butylphosphine tetrafluoroborate (101 mg, 0.26 mmol), potassium *tert*-butoxide (384 mg, 4 mmol) were added to a oven dried two-necked flask equipped with a magnetic stir bar and a condenser. The flask was then evacuated and backfilled with argon, this evacuation and backfill procedure was

repeated twice. Then 15 mL toluene was added under argon atmosphere. The mixture was then stirred under reflux at 110°C for 24 h. As the mixture was cooled down to room temperature, the reaction solution was transferred into a separatory funnel and then neutralized with anhydrous sodium sulfate. After filtration and concentration under reduced pressure, the crude product was purified by column chromatography with dichloromethane/petroleum ether (v/v=1/1) as eluent to give the title compound as green powder (0.52 g, yield: 59%). ¹H NMR (CDCl₃, 500 MHz) δ (ppm): 7.79 (2 H, d, *J* 8.5), 7.58 (2 H, d, *J* 8.5), 7.48 (2 H, dd, *J* 7.7, 1.5), 7.07 - 6.93 (4 H, m), 6.35 (2 H, dd, *J* 8.1, 1.1), 2.92 (6 H, s), 1.69 (6 H, s). ¹³C NMR (126 MHz, CDCl₃) δ (ppm): 165.37 (s), 155.93 (s), 144.19 (s), 140.51 (s), 132.53 (s), 131.87 (s), 131.40 (s), 130.69 (s), 126.61 (s), 125.25 (s), 121.18 (s), 115.13 (s), 114.39 (s), 107.35 (s), 36.09 (s), 30.96 (s), 24.79 (s). MALDI-TOF-MS(M): *m/z* 441.2 [M+H]⁺. Anal. calcd for C₃₀H₂₄N₄(%): C 81.79, H 5.49, N 12.72; found: C 82.34, H 6.62, N 12.77.

Synthesis of 4-(4-(10*H*-phenoxazin-10-yl) phenyl) -2,6- dimethylpyridine -3,5-dicarbonitrile (Me-PXZ)

Me-PXZ was synthesized use the same reaction conduction with Me-DMAC between Me-Br and 10*H*-phenoxazine. The compound was yellow powder (Yield 70%). ¹H NMR (CDCl₃, 500 MHz) δ (ppm): 7.76 (2 H, d, *J* 8.5), 7.59 (2 H, d, *J* 8.4), 6.76 – 6.61 (6 H, m), 6.01 (2 H, dd, *J* 7.8, 1.5), 2.91 (6 H, s). ¹³C NMR (126 MHz, CDCl₃) δ (ppm): 165.40, 155.74, 144.01, 141.91, 133.71, 132.95, 131.75, 131.59, 123.49, 121.92, 115.70, 115.03, 113.45, 107.30, 24.78. MALDI-TOF-MS(M): *m/z* 415.3 [M+H]⁺. Anal. calcd for C₂₇H₁₈N₄O (%): C 78.24, H 4.38, N 13.52; found: C 79.17, H 4.79, N

13.68.

Exciton Lifetime and Rate Constant

The rate constants of ISC (k_{ISC}) and RISC (k_{RISC}) of three emitters based on the following equations:

$$k_p = \frac{1}{\tau_p} \quad (1)$$

$$k_d = \frac{1}{\tau_d} \quad (2)$$

$$k_{r,s} = \Phi_p k_p + \Phi_d k_d \approx \Phi_p k_p \quad (3)$$

$$k_{RISC} \approx \frac{k_p k_d \Phi}{k_{r,s}} \quad (4)$$

$$k_{ISC} \approx \frac{k_p k_d \Phi_d}{k_{RISC} \Phi_p} \quad (5)$$

In this study, the prompt PLQY (Φ_p) and delayed PLQY (Φ_d) were determined by using the total PLQY and the integrated intensity ratio between prompt and delayed components which was calculated from transient photoluminescence measurements. The intensity ratio between prompt (r_p) and delayed (r_d) components were determined using two fluorescent lifetimes (τ_p , τ_d) and fitting parameter (A_p , A_d) as follow.

$$I(t) = A_p e^{-\frac{t}{\tau_p}} + A_d e^{-\frac{t}{\tau_d}} \quad (6)$$

$$r_p = \frac{A_p \tau_p}{A_p \tau_p + A_d \tau_d} \quad (7)$$

$$r_d = \frac{A_d \tau_d}{A_p \tau_p + A_d \tau_d} \quad (8)$$

Then, the prompt PLQY (Φ_p) and delayed PLQY (Φ_d) were determined using intensity ratio (r_p , r_d) and total PLQY.

$$\Phi_{total} = \Phi_p + \Phi_d \quad (9)$$

$$\Phi_p = r_p \Phi_{total} \quad (10)$$

$$\Phi_d = r_d \Phi_{total} \quad (11)$$

Supplementary Figures

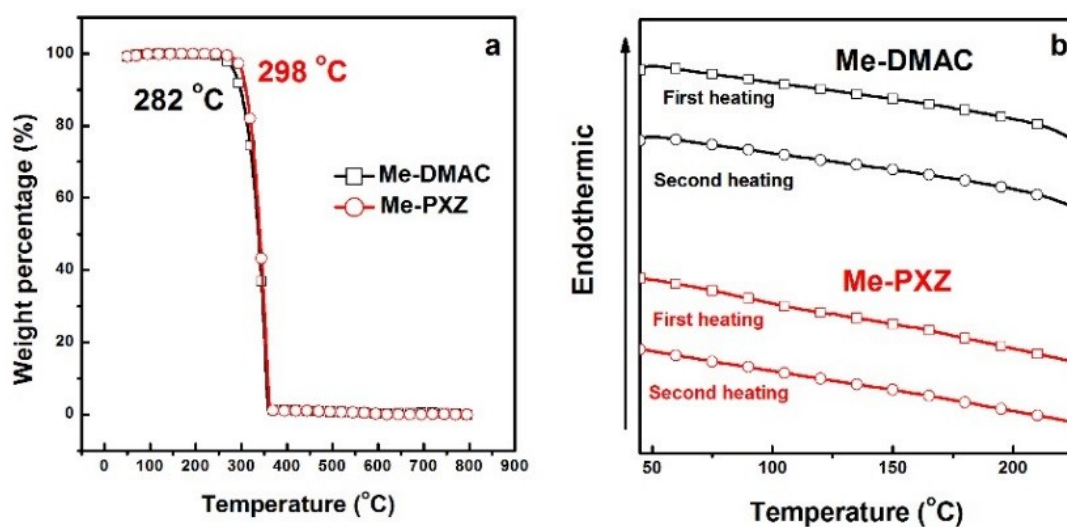


Figure S1 (a) TGA curve under N_2 with heating rate of 10 K/min, (b) First and second heating curve under N_2 with heating rate of 10 K/min.

Geometry

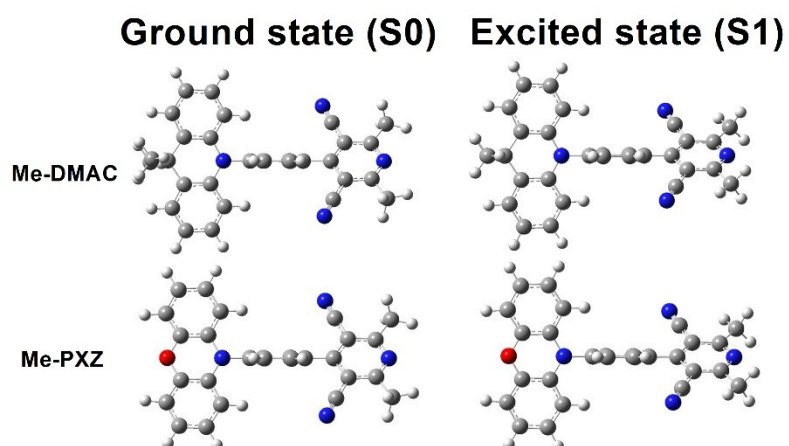


Figure S2 Optimized S0 and S1 geometry of Me-DMAC and Me-PXZ using B3LYP

under 6-31G** level. The torsion angle between 3,5-diCN-pyridine and the adjacent benzene are 54.1° and 53.6° for S0, 35.6° and 35.3° for S1, respectively.

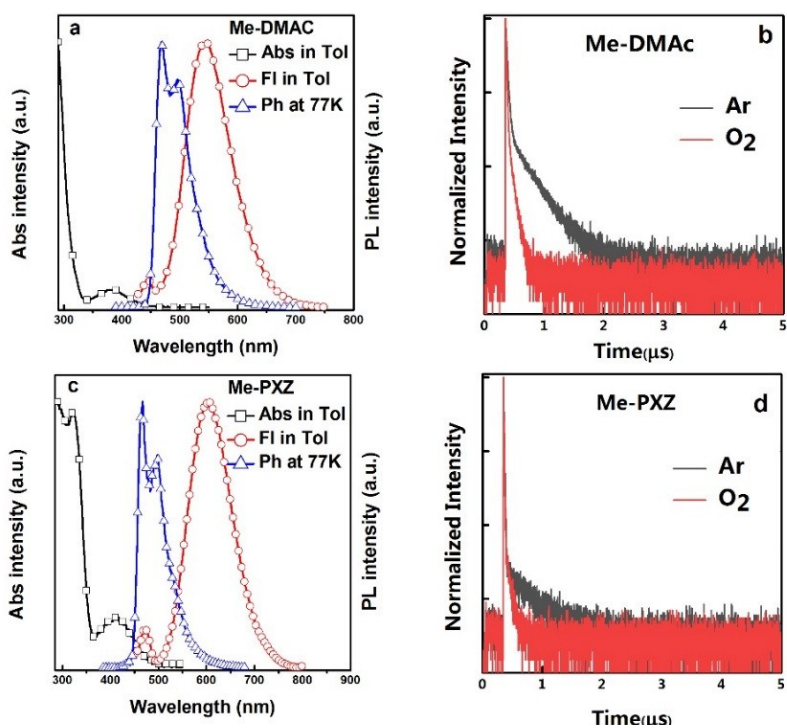


Figure S3 Photophysical properties of Me-DMAC and Me-PXZ in dilute toluene (10^{-4} M). Absorption, photoluminescence at R.T. and phosphorescence at 77K of (a) Me-DMAC, (c) Me-PXZ. Transient PL spectra under Ar and bubbled with O_2 of (b) Me-DMAC, (d) Me-PXZ.

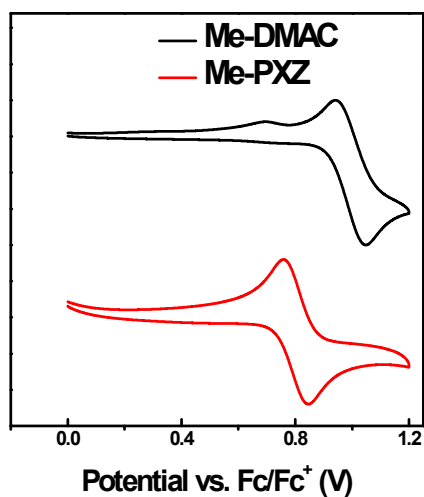
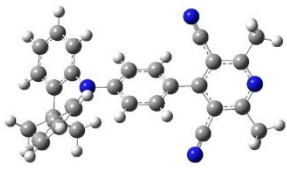
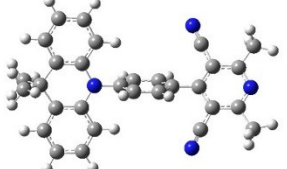


Figure S4 The cyclic voltammetry curves in acetonitrile/ CH_2Cl_2 of Me-DMAC and Me-PXZ.

Compounds	QA	QE
Me-DMAC		
Energy(a.u.)	-1376.687	-1376.189

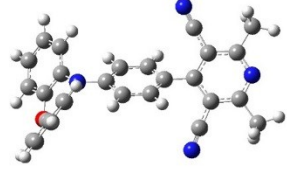
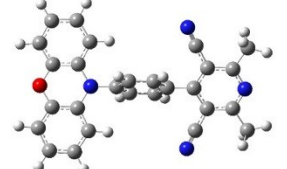
Compounds	QA	QE
Me-PXZ		
Energy(a.u.)	-1333.949	-1333.953

Figure S5 theoretical geometries of QA and QE conformation of Me-DMAC and Me-PXZ understand B3LYP /6-31G** level.

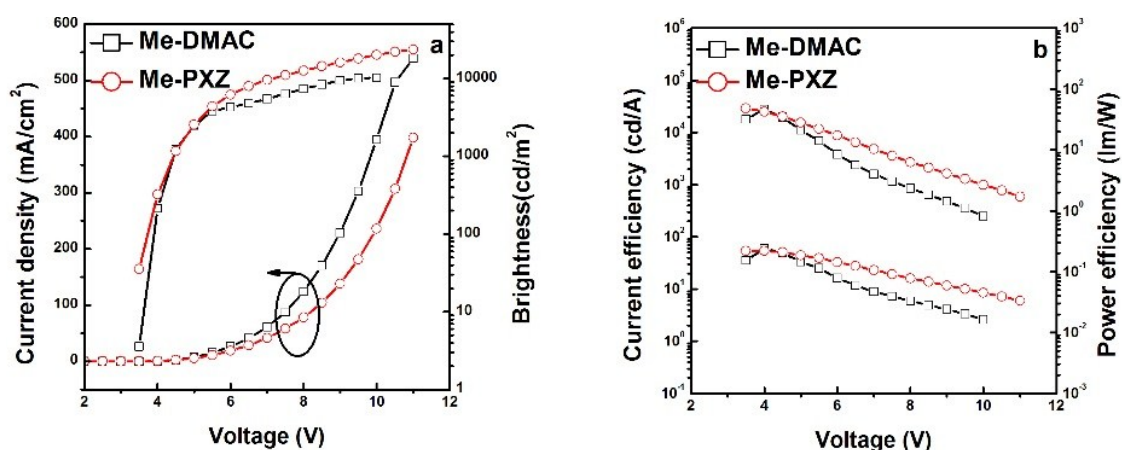


Figure S6 EL properties of doping devices based Me-DMAC and Me-PXZ. (a) Current-Voltage-Brightness (J-V-L) curves, (b) Current efficiency-Voltage-Power efficiency

curves.

Tab. S1 Calculated Oscillator strengths (f) at PBE0/def2-SVP level with Nuclear Ensemble Approach.

Compound	f
Me-DMAC	0.007230
Me-PXZ	0.006414